



Published in final edited form as:

*J Membr Biol.* 2013 December ; 246(12): 915–926. doi:10.1007/s00232-013-9593-0.

## Relative CO<sub>2</sub>/NH<sub>3</sub> permeabilities of human RhAG, RhBG, and RhCG

R. Ryan Geyer<sup>2</sup>, Mark D. Parker<sup>2</sup>, Ashley M. Toye<sup>3</sup>, Walter F. Boron<sup>2</sup>, Raif Musa-Aziz<sup>1,2</sup>

<sup>1</sup>Department of Physiology and Biophysics, University of Sao Paulo, Sao Paulo, 05508-000, Brazil,

<sup>2</sup>Department of Physiology and Biophysics, Case Western Reserve University School of Medicine, Cleveland, OH 44106, USA,

<sup>3</sup>University of Bristol, School of Biochemistry, Medical Science Building, Bristol, United Kingdom.

### Abstract

Mammalian glycosylated rhesus (Rh) proteins include the erythroid RhAG and the non-erythroid RhBG and RhCG. RhBG and RhCG are expressed in multiple tissues, including hepatocytes and the collecting duct (CD) of the kidney. Here we expressed human RhAG, RhBG, and RhCG in *Xenopus* oocytes (vs. H<sub>2</sub>O-injected control oocytes) and used microelectrodes to monitor the maximum transient change in surface pH ( $\Delta \text{pH}_S$ ) caused by exposing the same oocyte to 5% CO<sub>2</sub>/33 mM HCO<sub>3</sub><sup>-</sup> (an increase) or 0.5 mM NH<sub>3</sub>/NH<sub>4</sub><sup>+</sup> (a decrease). Subtracting the respective values for day-matched, H<sub>2</sub>O-injected control oocytes yielded channel-specific values (\*). ( $\Delta \text{pH}_S^*$ )<sub>CO<sub>2</sub></sub> and ( $-\Delta \text{pH}_S^*$ )<sub>NH<sub>3</sub></sub> were each significantly > 0 for all channels, indicating that RhBG and RhCG—like RhAG—can carry CO<sub>2</sub> and NH<sub>3</sub>. We also investigated the role of a conserved aspartate residue, which was reported to inhibit NH<sub>3</sub> transport. However, surface biotinylation experiments indicate the mutants RhBG<sub>D178N</sub> and RhCG<sub>D177N</sub> have at most a very low abundance in the oocyte plasma membrane. We demonstrate for the first time that RhBG and RhCG—like RhAG—have significant CO<sub>2</sub> permeability, and we confirm that RhAG, RhBG, and RhCG all have significant NH<sub>3</sub> permeability. However, as evidenced by ( $\Delta \text{pH}_S^*$ )<sub>CO<sub>2</sub></sub>/( $-\Delta \text{pH}_S^*$ )<sub>NH<sub>3</sub></sub> values, we could not distinguish among the CO<sub>2</sub>/NH<sub>3</sub> permeability ratios for RhAG, RhBG, and RhCG. Finally, we propose a mechanism whereby RhBG and RhCG contribute to acid secretion in the CD by enhancing not only the transport of NH<sub>3</sub> but also the transport of CO<sub>2</sub> across the membranes of CD cells.

### Keywords

gas channels; Rhesus protein; biotinylation; surface pH; collecting duct

## INTRODUCTION

The regulation of blood pH within the normal range (7.35–7.45) is one of the most important physiological processes because the structure and function of virtually all proteins are directly influenced by pH.

With a person on a typical Western diet, cellular metabolism produces ~40 mmol of net  $H^+$ /day (Giebisch and Windhager 2009). In addition, the transfer of dietary  $H^+$  from the gastrointestinal tract to the extracellular fluid, as well as the obligatory loss of alkali in stool, represents a net gain of an additional 30 mmol of  $H^+$ /day (Giebisch and Windhager 2009). The total daily  $H^+$  load of ~70 mmol titrates ~70 mmol of  $HCO_3^-$  from body fluids to produce  $CO_2$  (which the lungs excrete) and  $H_2O$ . If the  $HCO_3^-$  consumed in this buffer reaction were not constantly replenished, a catastrophic metabolic acidosis would ensue. To maintain plasma  $[HCO_3^-]$  and thus pH, the kidney—operating in a steady state—must perform three related tasks. [1] Reabsorb the ~4000 mmol/day of  $HCO_3^-$  filtered in the glomeruli; this operation merely prevents the loss of  $HCO_3^-$  into the urine. [2] Transfer to the blood plasma an additional ~70 mmol/day of “new”  $HCO_3^-$  to replenish the  $HCO_3^-$  lost to  $H^+$  buffering. And [3] secrete into the tubule lumen ~70 mmol/day of  $H^+$  that is produced during the process of generating the “new”  $HCO_3^-$ . Virtually all of the secreted  $H^+$  titrates buffers that increase the  $H^+$ -carrying capacity of the tubule fluid.

The most important of these urinary buffers is  $NH_3/NH_4^+$ , nearly all of which is synthesized de novo by the proximal tubule (PT). Deamidation of glutamine to glutamate and then  $\alpha$ -ketoglutarate in the PT mitochondria yields two molecules of  $NH_4^+$ . Metabolism of  $\alpha$ -ketoglutarate generates two  $HCO_3^-$  ions, which exit the cell across the basolateral membrane via the  $Na/HCO_3^-$  cotransporter (NBCe1-A; (Boron and Boulpaep 1983; Romero et al. 1997) for entry into the blood. The newly formed  $NH_4^+$  dissociates in the PT cell to form  $NH_3$  and  $H^+$ . The  $NH_3$  exits across the apical membrane of the cell—probably at least in part via AQP1 (Nakhoul et al. 2001; Musa-Aziz et al. 2009a)—entering the tubule lumen. There the  $NH_3$  reacts with  $H^+$ —secreted mainly via the Na-H exchanger NHE3 (Nagami 1988)—to reform  $NH_4^+$ . The medullary thick ascending limb (mTAL) reabsorbs much of the  $NH_4^+$ , which—as considered in the Discussion—eventually enters the lumen of the collecting duct in a complex series of events.

From the above discussion, it is clear that the net movement of  $NH_3/NH_4^+$  from the TAL lumen to the CD lumen is critical. Four lines of evidence suggest that the Rh glycoproteins RhBG and RhCG make a substantial contribution to the movement of  $NH_3$  across the membranes of the CD cells:

1. In heterologous expression systems RhBG and RhCG both transport  $NH_3$  (Bakouh et al. 2006; Mak et al. 2006; Weiner and Verlander 2010).
2. In the kidney, RhBG and RhCG are expressed mainly in the CD  $\alpha$ -intercalated cells (Eladari et al. 2002; Quentin et al. 2003; Verlander et al. 2003; Seshadri et al. 2006; Biver et al. 2008; Brown et al. 2009), far more so than in principal cells (Seshadri et al. 2006). RhBG is expressed only in the basolateral membrane (Quentin et al. 2003; Verlander et al. 2003; Han et al. 2006; Kim et al. 2009),

whereas RhCG is expressed both in the basolateral (Han et al. 2006; Seshadri et al. 2006; Brown et al. 2009; Kim et al. 2009) and apical membranes (Eladari et al. 2002; Quentin et al. 2003; Verlander et al. 2003; Han et al. 2006; Seshadri et al. 2006; Biver et al. 2008; Brown et al. 2009; Kim et al. 2009).

3. In response to chronic metabolic acidosis, wild-type (WT) mice increase RhBG (Bishop et al. 2010) and RhCG (Seshadri et al. 2006) protein abundance, consistent with a role in support of acid excretion.
4. When subjected to chronic metabolic acidosis, mice with intercalated-cell-specific knockouts of RhBG (Bishop et al. 2010) or RhCG (Lee et al. 2010) transiently excrete less urinary  $\text{NH}_3/\text{NH}_4^+$  than WT mice.

Previous work shows that the Rh glycoprotein related to RhBG and RhCG—namely, RhAG—transports not only  $\text{NH}_3$  (Ripoche et al. 2006; Musa-Aziz et al. 2009a) but also  $\text{CO}_2$  (Endeward et al. 2008; Musa-Aziz et al. 2009a). Moreover, when compared to the bacterial Rh protein AmtB and various mammalian aquaporins, RhAG exhibits a characteristic selectivity for  $\text{NH}_3$  vs.  $\text{CO}_2$  (Musa-Aziz et al. 2009a; Geyer et al. 2013b). Thus, important questions are whether RhBG and RhCG also conduct  $\text{CO}_2$  and, if so, how the  $\text{CO}_2/\text{NH}_3$  selectivities of RhBG and RhCG compare to those of AQP and other Rh proteins. In the present study we express RhBG, RhCG, or—as a control—RhAG in *Xenopus* oocytes and use microelectrodes to monitor the transient changes in cell-surface pH ( $\text{pH}_s$ ) as we expose cells to  $\text{CO}_2$  or  $\text{NH}_3$ . The maximal excursions of  $\text{pH}_s$  ( $\Delta \text{pH}_s$ ) are semiquantitative indices of  $\text{CO}_2$  and  $\text{NH}_3$  permeability. We find that both RhBG and RhCG conduct  $\text{CO}_2$  and  $\text{NH}_3$ . However, the  $\text{CO}_2/\text{NH}_3$  permeability ratios for RhAG, RhBG, and RhCG were indistinguishable from one another. Based on our results, we propose a model whereby basolateral RhBG and RhCG, not only enhance the uptake of  $\text{NH}_3$  (Mak et al. 2006; Kim et al. 2009; Wagner et al. 2009; Gruswitz et al. 2010) but also of  $\text{CO}_2$  across the basolateral membranes of the CD cells. This  $\text{CO}_2$  uptake would be anticipated to promote basolateral  $\text{Cl}^-/\text{HCO}_3^-$  exchange and thus help drive  $\text{H}^+$  secretion into the CD lumen.

## MATERIALS AND METHODS

### Expression in *Xenopus* oocytes

**cDNA clones.**—RhAG and the *Xenopus* expression vector BSXG have been described previously (Bruce et al. 2009). BSXG-RhBG and RhCG were generated from pGFPC1-RhBG and pGFPC1-RhCG constructs (Brown et al. 2009) by double restriction digest, using *Bgl*III and *Xma*I and ligated into *Bgl*III and *Xma*I pre-cut BSXG4 vector. The site-directed mutants RhBG<sub>D178N</sub> and RhCG<sub>D177N</sub> were generated using the QuikChange Site-Directed Mutagenesis Kit (Catalog # 200518, Stratagene, Cedar Creek, TX) according to the manufacturer's protocol. The sequence of all clones was confirmed by DNA sequencing (Eurofin MWG Operon, UK and Keck DNA Sequencing Facility, New Haven, CT).

**cRNA synthesis.**—The restriction enzyme *Xho*I was used to linearize the pBSXG plasmid containing human RhBG, RhBG<sub>D178N</sub>, RhCG, or RhCG<sub>D177N</sub> cDNAs. The linearized cDNAs were then purified using the QIAquick PCR purification kit (Qiagen Inc., Valencia, CA). Transcribed, capped cRNA was generated using the T7 mMessage

mMachine kit (Ambion, Austin, TX) and these cRNAs were purified and concentrated using the RNeasy MinElute RNA Cleanup Kit (Qiagen).

**Xenopus oocyte isolation.**—Oocytes were isolated from female *Xenopus laevis* frogs according to methods described previously (Musa-Aziz et al. 2010). Briefly, we surgically removed ovaries from frogs anesthetized in 0.2% MS-222 (Ethyl 3-aminobenzoate methanesulfonate, Sigma-Aldrich, St. Louis, MO). The ovarian lobes were dissected into small pieces and washed in 0-Ca solution (in mM: 98 NaCl, 2 KCl, 1 MgCl<sub>2</sub>, 5 HEPES, pH 7.5, osmolality 195 mOsm/kg) prior to enzymatic defolliculation with 2 mg/mL type IA collagenase (Sigma-Aldrich) in 0-Ca. Stage V–VI oocytes were selected and stored at 18°C in filter-sterilized OR3 medium that contained (per 2 liters) one pack of powdered Leibovitz L-15 media (13.7 g/pack) with L-glutamine (GIBCO-BRL), 100 mL of 10,000 U/mL penicillin, 10,000 U/mL streptomycin solution (Sigma-Aldrich), and 5 mM HEPES titrated to pH 7.5, osmolality ~195 mOsm/kg H<sub>2</sub>O until use.

**Microinjection of cRNAs.**—One day after isolation, oocytes were injected with either 25 ng of cRNA encoding human RhBG, RhBG<sub>D178N</sub>, RhCG, or RhCG<sub>D177N</sub> cRNA (delivered as 25 nL of a 1 ng/nL cRNA solution) or 25 nL of sterile water (Ambion) for control H<sub>2</sub>O-injected oocytes. After injection, we stored oocytes at 18°C in OR3 medium for 4–5 days before using them in experiments.

### Protein expression measurements

**Biotinylation.**—Biotinylation of plasma-membrane resident proteins was performed using the EZ-Link Sulfo-NHS-Biotinylation Kit (part # 21425, Thermo Fisher Scientific, Rockford, IL) according to the manufacturers recommendations, with some previously described modifications (Geyer et al. 2013a; Geyer et al. 2013b). Briefly, groups of 30 oocytes were incubated with Sulfo-NHS-Biotin biotinylation reagent at 4°C × 1 h. The biotinylation reaction was terminated by adding the supplied quenching buffer and washing the cells in TBS. Cells were lysed by trituration in Lysis buffer (TBS that contained 1% Triton X100 and a cOmplete EDTA-free protease inhibitor tablet; part # 11873580001; Roche, Indianapolis, IN). The insoluble fraction was pelleted by centrifugation and a sample of the supernatant containing solubilized protein (“total protein” fraction) was set aside for western-blot analysis. Biotinylated protein was isolated from the remainder of the solubilized fraction by an incubation at RT × 1 h with immobilized NeutrAvidin gel. Non-biotinylated protein was rinsed from the gel by repeated washing with lysis buffer. Biotinylated protein was subsequently eluted from the gel using 300 µl of 1 × SDS sample buffer (Invitrogen, Carlsbad, CA) containing 50 mM DTT (“biotinylated protein” fraction).

**Western-blot analysis.**—Total and biotinylated protein samples were separated by SDS-PAGE on 12% Tris-Glycine gels (Invitrogen). The samples were transferred to PVDF membranes using the iBlot apparatus (Invitrogen) × 8 min. The membranes were rinsed with TBST (Tris-buffered saline/Tween, in mM: 50 Tris-Base, 150 NaCl, pH 7.4, 0.1% Tween 20 [#P7949, Sigma-Aldrich]) and then transferred to TBST plus 5% powdered milk. The membranes were probed with one of a number of rabbit primary C-terminal polyclonal antibodies raised against human RhAG (Toye et al. 2008), RhBG or RhCG (Brown et al.

2009), followed by a goat anti-rabbit secondary monoclonal antibody (# AP132P; Millipore, Billerica, MA), and detected using ECL plus Western Blotting Detection Reagents (GE Healthcare Life Sciences, Pittsburgh, PA).

### Electrophysiological measurements

**Chamber.**—Oocytes were placed in plastic perfusion chamber, with a channel 3 mm wide  $\times$  30 mm long; saline constantly flowed down this channel at a rate of 4 mL/min. Perfusing solutions were delivered using syringe pumps (Harvard Apparatus, South Natick, MA). Switching between solutions was performed by pneumatically operated valves (Clippard Instrument Laboratory, Cincinnati, OH). All experiments were performed at room temperature ( $\sim 22^{\circ}\text{C}$ ).

**Transport Assay Solutions.**—The ND96 solution contained in mM: 96 NaCl, 2 KCl, 1  $\text{MgCl}_2$ , 1.8  $\text{CaCl}_2$ , and 5 HEPES, pH 7.50, osmolality 195 mOsm. The  $\text{CO}_2/\text{HCO}_3^-$  solution was identical to ND96 except that 33 mM  $\text{NaHCO}_3$  replaced 33 mM NaCl, and the solution was bubbled with 5%  $\text{CO}_2$ /balanced  $\text{O}_2$ . The 0.5 mM  $\text{NH}_3/\text{NH}_4^+$  solution was made by first replacing 5 mM NaCl with 5 mM  $\text{NH}_3/\text{NH}_4^+$  and then diluted the solution 1:10 with standard ND96 solution.

**Measurement of surface pH.**—Our approach for monitoring surface pH ( $\text{pH}_\text{S}$ ) of an oocyte has been described in detail elsewhere (Musa-Aziz et al. 2009a; Geyer et al. 2013b). We measured  $\text{pH}_\text{S}$  using a pH-electrode with a tip diameter of  $\sim 15\text{ }\mu\text{m}$ , which was filled with  $\text{H}^+$  ionophore mixture B (# 95293 Fluka Chemical Corp., Ronkonkoma, NY), and amplified by a FD223 electrometer (World Precision Instruments, Inc., Sarasota, FL). The external reference electrode for the  $\text{pH}_\text{S}$  measurements was a calomel half-cell (connected to a model 750 electrometer, World Precision Instruments) contacting a 3M-KCl-filled micropipette, which contacted the fluid in the chamber. We also recorded  $\text{pH}_\text{i}$  and  $V_\text{m}$  in each experiment, as described previously (Musa-Aziz et al. 2009a; Musa-Aziz et al. 2009b), but do not report these data. The analog subtraction of the calomel-electrode signal from the  $\text{pH}_\text{S}$ -electrode signal produced the signal due to  $\text{pH}_\text{S}$ . We used an ultra-fine micromanipulator (model MPC-200 system, Sutter Instrument Company, Novato, CA) to position the  $\text{pH}_\text{S}$ -electrode tip at the surface of the oocyte, and then to advance it  $\sim 40\text{ }\mu\text{m}$  further, forming a slight dimple in the membrane. For routine recalibration of the electrode, we periodically withdrew the electrode from the surface of the oocyte and positioned it in the bulk extracellular fluid (BECF, pH 7.50). The tip of the  $\text{pH}_\text{S}$  microelectrode, with respect to the flow of solution, was positioned near the oocyte's equator, in the "shadow" of the oocyte.

### Analysis of $\text{pH}_\text{S}$ data

We used an approach described previously (Endeward et al. 2006; Musa-Aziz et al. 2009a; Musa-Aziz et al. 2009b) to compute the maximum magnitude (i.e., "spike height" or  $\text{pH}_\text{S}$ ) of the  $\text{pH}_\text{S}$  transient elicited by applying a solution containing either extracellular 5%  $\text{CO}_2/\text{HCO}_3^-$  or 0.5 mM  $\text{NH}_3/\text{NH}_4^+$ . In brief, we determined the initial  $\text{pH}_\text{S}$ —before the application of  $\text{CO}_2/\text{HCO}_3^-$  or  $\text{NH}_3/\text{NH}_4^+$ —by comparing the  $\text{pH}_\text{S}$ -electrode voltage signal when the electrode tip was at the oocyte surface with the voltage signal obtained when the tip was in BECF lacking  $\text{CO}_2/\text{HCO}_3^-$  and  $\text{NH}_3/\text{NH}_4^+$  (7.50). We determined the maximum

pH<sub>S</sub> during exposure to CO<sub>2</sub>/HCO<sub>3</sub><sup>−</sup>, or the minimum pH<sub>S</sub> during exposure to NH<sub>3</sub>/NH<sub>4</sub><sup>+</sup> by comparing the voltage signal (at a time corresponding to the extreme pH<sub>S</sub> value) when the electrode tip was at the oocyte surface with the voltage signal obtained a few minutes later, when the tip was in the BECF containing CO<sub>2</sub>/HCO<sub>3</sub><sup>−</sup> or NH<sub>3</sub>/NH<sub>4</sub><sup>+</sup> (7.50). pH<sub>S</sub> is the algebraic difference between the extreme and initial pH values. All oocytes used in this study had initial  $V_m$  values at least as negative as −40 mV.

### In vitro assay of carbonic-anhydrase activity

To determine carbonic anhydrase (CA) activity, we used a colorimetric assay—conducted at 0°C—to monitor a fall in pH (Brion et al. 1988; Musa-Aziz et al. 2009a). The sample mixture consisted of 10 µl of protein (20 µg) from a membrane preparation of oocytes injected with cRNA (25 ng) encoding human CA IV, RhAG, RhBG or RhCG, plus 185 µl H<sub>2</sub>O and 5 µl of 1-octanol, for a total volume of 200 µl. In some experiments, we reduced the amount of injected hCA IV to 0.25 µg. We bubbled the sample mixture with 100% CO<sub>2</sub>, and then added 200 µl of buffer/indicator mix (5.0 mM Tris·HCl, 20 mM imidazole, and 0.4 mM para-nitrophenol, pH 8.00), thereby reducing [CO<sub>2</sub>] by half. The color of this CO<sub>2</sub>-rich solution was initially yellow, indicating a relatively alkaline solution. A yellow-to-clear color change—due to the reaction CO<sub>2</sub> + H<sub>2</sub>O → HCO<sub>3</sub><sup>−</sup> + H<sup>+</sup>—indicates the reaction endpoint. We used a stopwatch to measure the time to achieve the endpoint. Protein concentrations of samples were determined using an assay from Pierce (Pierce® BCA Protein Assay Kit, Thermo Scientific).

### Statistics

Data are presented as mean ± SEM. To compare the difference between two means, we performed Student's *t* tests (two tails). To compare more than two means, we performed a 1-way ANOVA followed by a Student–Newman–Keuls posthoc analysis, using KaleidaGraph (Version 4, Synergy Software). *P* < 0.05 was considered significant.

## RESULTS

Our goal was to use pH<sub>S</sub> measurements to determine whether—like RhAG—RhBG and RhCG are permeable both to CO<sub>2</sub> and NH<sub>3</sub>. We examined not only the WT proteins but also constructs in which we mutated a highly conserved Asp residue to Asn (Figure 1).

### pH<sub>S</sub> transients induced by CO<sub>2</sub> entry

**Oocytes injected with H<sub>2</sub>O.**—When we add CO<sub>2</sub>/HCO<sub>3</sub><sup>−</sup> to bulk extracellular fluid, then—if the influx of CO<sub>2</sub> dominates over the entry of HCO<sub>3</sub><sup>−</sup> in terms of pH<sub>S</sub> changes—the entry of CO<sub>2</sub> into the cell creates a deficit of CO<sub>2</sub> near the outer surface of the membrane (Figure 2a: left side). CO<sub>2</sub> diffusion from the BECF partially replenishes the deficit. However, additional replenishment occurs via the following reactions at the outer surface of the cell: HCO<sub>3</sub><sup>−</sup> + H<sup>+</sup> → H<sub>2</sub>CO<sub>3</sub> → H<sub>2</sub>O + CO<sub>2</sub>. The result is the consumption of protons and thus a rapid rise—or ‘spike’—in pH<sub>S</sub> that decays exponentially from its peak towards pH<sub>Bulk</sub> as the CO<sub>2</sub> influx gradually slows. The light gray record on the left side of Figure 2b shows the pH<sub>S</sub> trajectory for a H<sub>2</sub>O-injected oocyte (replicated in Figure 2c–d). The maximal pH<sub>S</sub> spike height (pH<sub>S</sub>) is a semi-quantitative index of the rate of CO<sub>2</sub> entry. Thus, other



things being equal,  $pH_S$  is an index of the permeability to  $CO_2$ , although the relationship between  $pH_S$  and permeability is not expected to be linear (Somersalo et al. 2012).

**Oocytes expressing RhAG.**—The left side of Figure 2b also shows the effect of expressing RhAG on the  $pH_S$  trajectory elicited by an exposure to  $CO_2$  (black record). As was the case with the  $H_2O$ -injected oocyte, the exposure to  $CO_2/HCO_3^-$  causes a rapid rise in  $pH_S$ , followed by an exponential decay. However, the expression of RhAG increases the magnitude of  $pH_S$  compared to day-matched  $H_2O$ -injected control oocyte. Thus, RhAG increases the  $CO_2$  permeability of the oocyte, consistent with the earlier work of Musa Aziz *et al.* (Musa-Aziz et al. 2009a).

**Oocytes expressing RhBG.**—The left side of Figure 2c (black record) shows that expressing RhBG produces a  $CO_2$ -induced  $pH_S$  trajectory that is similar to that observed above with RhAG. On the other hand, with an oocyte expressing RhBG<sub>D178N</sub> (Figure 2c: gray record), the magnitude of  $pH_S$  is only slightly greater than that of the day-matched  $H_2O$ -injected oocyte.

**Oocytes expressing RhCG.**—The left side of Figure 2d (black record) shows that an oocyte expressing RhCG, likewise, exhibits a much greater  $pH_S$  than the day-matched  $H_2O$ -injected control. On other hand, the oocyte expressing RhCG<sub>D177N</sub> (gray record)—like the one expressing RhBG<sub>D178N</sub>—produces a  $pH_S$  trajectory that is indistinguishable from that of the  $H_2O$ -injected control oocyte.

### **$pH_S$ transients induced by $NH_3$ entry**

**Oocytes injected with  $H_2O$ .**—When we add  $NH_3/NH_4^+$  to the BECF, then—if the entry of  $NH_3$  dominates over the entry of  $NH_4^+$  in terms of  $pH_S$  changes—the influx of  $NH_3$  creates a deficit in  $NH_3$  at the outer surface of the cell membrane (Figure 2a: right side). Diffusion of  $NH_3$  from the BECF partially replenishes the deficit. However, the  $NH_3$  deficit is also replenished by the following reaction at the outer surface of the cell:  $NH_4^+ \rightarrow NH_3 + H^+$ . This results in the production of protons and thus a rapid fall in  $pH_S$  that decays towards  $pH_{Bulk}$  as the  $NH_3$  influx gradually slows. The light gray record on the right side of Figure 2b (replicated in Figure 2c–d) illustrates the  $pH_S$  trajectory for a  $H_2O$ -injected oocyte. The maximum  $pH_S$  spike depth  $pH_S$  is a semi-quantitative index of the rate of  $NH_3$  entry. Thus,  $(-pH_S)$  reflects the permeability to  $NH_3$ .

**Oocytes expressing RhAG.**—The right side of Figure 2b (black record) shows the effect of expressing RhAG on the  $pH_S$  changes induced by exposing the cell to  $NH_3$ . As we saw with the  $H_2O$ -injected oocyte above, the  $NH_3/NH_4^+$  exposure causes a rapid  $pH_S$  decrease and a slower decay. However, the magnitude of  $pH_S$  is substantially greater for the RhAG-expressing oocyte as compared to the  $H_2O$ -injected oocyte. These results confirm the results of others (Ripoche et al. 2004; Ripoche et al. 2006) and of Musa-Aziz et al. (2009a) that RhAG is an  $NH_3$  channel.

**Oocytes expressing RhBG.**—Previous studies, using methodologies different from those presented in the present work, have demonstrated that RhBG transports  $NH_3$  (Ludewig

2004; Zidi-Yahiaoui et al. 2005; Mak et al. 2006). The right side of Figure 2c (black record) shows that an oocyte expressing RhBG responds to  $\text{NH}_3$  in much the same way as an oocyte expressing RhAG, with a large ( $-\text{pH}_\text{S}$ ) indicative of  $\text{NH}_3$  permeability. As we saw with  $\text{CO}_2$ , the oocyte expressing RhBG<sub>D178N</sub> has a  $\text{pH}_\text{S}$  response that is very similar to that of a  $\text{H}_2\text{O}$ -injected oocyte when exposed to  $\text{NH}_3/\text{NH}_4^+$  (Figure 2c: gray record).

**Oocytes expressing RhCG.**—As is the case for RhBG, the  $\text{NH}_3$  permeability of RhCG has been reported (Ludewig 2004; Zidi-Yahiaoui et al. 2005; Bakouh et al. 2006; Mak et al. 2006), though using  $\text{pH}_\text{i}$  monitoring. The right side of Figure 2d (black record) confirms that RhCG is an effective  $\text{NH}_3$  channel. However, in the oocyte expressing RhCG<sub>D177N</sub>, an exposure to  $\text{NH}_3/\text{NH}_4^+$  elicits a  $\text{pH}_\text{S}$  response that is very similar to that of the day-matched  $\text{H}_2\text{O}$ -injected oocyte (Figure 2d: gray record).

Although not shown, our recordings of  $V_\text{m}$  reveal no evidence of an electrogenic flux of  $\text{NH}_4^+$ .

Taken together, our data indicate that the WT proteins RhAG, RhBG, and RhCG all transport both  $\text{CO}_2$  and  $\text{NH}_3$ .

### Analysis of surface expression

It has been proposed by Gruswitz et al. (2010) that these conserved Asp residues—D178N in RhBG and D177N in RhCG—serves to stabilize these Rh proteins. If the D-to-N mutations destabilize RhBG and RhCG, then it is possible that the oocyte synthesizes but rapidly degrades the mutants, fails to traffic the mutant to the plasma membrane at a normal rate, or retrieves the mutant from the plasma membrane at an excessive rate. In any case, the surface abundance of the mutant proteins would be low. To investigate the extent to which the low functional expression of RhBG<sub>D178N</sub> and RhCG<sub>D177N</sub> reflects a low plasma-membrane abundance, we biotinylated oocytes expressing RhAG, RhBG, RhBG<sub>D178N</sub>, RhCG, and RhCG<sub>D177N</sub>, and performed western blotting of both the total protein fraction and the biotinylated (i.e., plasma-membrane-resident) protein fractions using previously described polyclonal C-terminal RhAG, RhBG and RhCG antibodies.

Figure 3a is a western blot that shows the total and surface expression of RhAG. The band at ~38 kDa represents the unglycosylated or core-glycosylated protein, whereas the immunoreactive higher molecular weight pattern centered around 50 kDa is consistent with mature N-linked glycosylated protein. Based on such blots, we estimate that a substantial proportion of the total RhAG expression is resident in the plasma-membrane fraction ( $44 \pm 3\%$ ,  $n = 4$ ), and that most of the surface protein has a mature glycosylation ( $70 \pm 9\%$ ,  $n = 4$ ).

Figure 3b is similar to Figure 3a except that it focuses on WT RhBG and RhBG<sub>D178N</sub>. The introduction of the D178N mutation substantially reduces total expression (in our experiments we estimate an average  $68 \pm 3\%$  reduction compared to wild-type,  $n=4$ ). Both WT and RhBG<sub>D178N</sub> are expressed to the plasma membrane:  $43 \pm 6\%$  ( $n=4$ ) of total in the case of WT and  $22 \pm 7\%$  ( $n=4$ ) for the mutant. An interesting observation is that virtually all of the RhBG<sub>D178N</sub> protein—both total and surface—is at a molecular weight consistent with unglycosylated or core-glycosylated protein.



Figure 3c is similar to Figure 3b except that it focuses on RhCG and RhCG<sub>D177N</sub>. We estimate that  $30 \pm 3\%$  ( $n=4$ ) of total WT RhCG protein is resident in the plasma-membrane fraction. On the other hand, RhCG<sub>D177N</sub> expression is barely detectable in either the total or plasma-membrane fractions. Thus, although injecting oocytes with cRNA encoding WT RhBG or RhCG results in the robust accumulation of the cognate protein in the plasma membrane, the injection of cRNA encoding the mutants RhBG<sub>D178N</sub> or RhCG<sub>D177N</sub> results in little protein in the plasma membrane.

### Summary of $pH_S$ data

Figure 4 summarizes the  $pH_S$  data for a larger number of experiments like those in Figure 2b–d. Here we ignore the two mutants, which were not appreciably present at the plasma membrane. We pair each oocyte expressing a WT channel with its day-matched, H<sub>2</sub>O-injected control. Figure 4a shows that the application of CO<sub>2</sub>/HCO<sub>3</sub><sup>−</sup> yields to a mean  $pH_S$  for RhAG, RhBG, or RhCG that is significantly greater than that for day-matched H<sub>2</sub>O-injected controls.

Figure 4b shows that the mean  $pH_S$  produced by the application of NH<sub>3</sub>/NH<sub>4</sub><sup>+</sup> for RhAG, RhBG, or RhCG is significantly greater than that for day-matched H<sub>2</sub>O-injected controls. These observations demonstrate that RhBG and RhCG—like RhAG—function not only as NH<sub>3</sub> channels but also as CO<sub>2</sub> channels.

### Channel-dependent gas transport

The portion of the CO<sub>2</sub>-induced  $pH_S$  signal that we can ascribe to a particular channel is the difference between the  $pH_S$  of each channel-expressing oocyte (e.g., black bars in Figure 4a) and the mean  $pH_S$  of the day-matched H<sub>2</sub>O-injected controls (e.g., light gray bars in Figure 4a). Figure 5a summarizes these differences, computed oocyte by oocyte, for the CO<sub>2</sub> data—the channel-dependent signal ( $pH_S^*$ )<sub>CO2</sub>. Similarly, Figure 5b summarizes the analogous differences for the NH<sub>3</sub> data—the channel-specific signal ( $pH_S^*$ )<sub>NH3</sub>. The six mean values—semiquantitative indices of channel-dependent gas permeability—are all significantly greater than zero. Note that the values in Figure 5 are not true permeabilities, but rather indices of relative CO<sub>2</sub> or NH<sub>3</sub> permeabilities, as determined by the product of intrinsic (or per-channel) gas conductance and the number of channels proteins in the plasma membrane.

### Ratios of indices of permeability—Gas Selectivity

In three previous studies, we have examined the relative CO<sub>2</sub>/NH<sub>3</sub> selectivities of the aquaporins 0–9 (Musa-Aziz et al. 2009a; Geyer et al. 2013b), RhAG (Musa-Aziz et al. 2009a), the bacterial Rh homolog AmtB (Musa-Aziz et al. 2009a), and the urea transporter UT-B (Geyer et al. 2013a). We found that each channel has a characteristic ratio ( $pH_S^*$ )<sub>CO2</sub>/( $pH_S^*$ )<sub>NH3</sub>, which is a relative index of the actual CO<sub>2</sub>/NH<sub>3</sub> permeability ratio. From the data that contribute to Figure 5, we can obtain similar information about RhBG and RhCG by dividing, oocyte by oocyte, ( $pH_S^*$ )<sub>CO2</sub> by the ( $pH_S^*$ )<sub>NH3</sub>—or conversely, dividing ( $pH_S^*$ )<sub>NH3</sub> by ( $pH_S^*$ )<sub>CO2</sub>. The numerical values in Figure 6 are not ratios of true permeabilities, but relative indices of CO<sub>2</sub>/NH<sub>3</sub> or NH<sub>3</sub>/CO<sub>2</sub> permeability ratios that we can compare from channel to channel if we obtain the data under identical

experimental conditions. Our 1-way ANOVA indicates no statistically significant difference among the ratios in Figure 6.

### Carbonic Anhydrase Activity

In principle, the enhanced  $\text{pH}_\text{S}$  spike produced by exposing Rh-expressing oocytes to  $\text{CO}_2$  (see left side of Figure 2b–d, and data summarized in Figure 4a and Figure 5a) could have been caused, not by  $\text{CO}_2$  conduction through the Rh protein, but by carbonic anhydrase (CA) activity in the Rh protein itself or an oocyte protein expressed in response to the Rh protein. To test the CA hypothesis, we injected oocytes with  $\text{H}_2\text{O}$  or with cRNA encoding CA IV (in which the catalytic domain is coupled via a GPI linkage to the outer surface of the membrane), RhAG, RhBG or RhCG. Previous work has shown that graded increases in the amount of injected cRNA encoding CA IV causes a graded increase in  $\text{pH}_\text{S}$  (see supplemental Fig 2 in (Musa-Aziz et al. 2009a)). Figure 7a shows that membrane preparations of oocytes injected with 12 ng CA IV cRNA/oocyte (we obtained similar results with 0.25 ng/oocyte; not shown)—compared to  $\text{H}_2\text{O}$  oocytes—require a much shorter time to achieve the pH endpoint in a colorimetric CA assay. However, membrane preparations of RhAG, RhBG or RhCG oocytes are indistinguishable from those of  $\text{H}_2\text{O}$ . Figure 7b–c show that oocytes from this preparation, when exposed to  $\text{CO}_2$  or  $\text{NH}_3$ , exhibited  $\text{pH}_\text{S}$  changes similar to those in Figure 5. Thus, we can rule out the hypothesis that the expression of RhAG, RhBG, or RhCG increase the size of  $\text{CO}_2$ -induced  $\text{pH}_\text{S}$  changes by engendering CA activity in either the cytosol or on the surface of the oocyte.

## DISCUSSION

### Overview

In the present study, we have made two main observations. First, we show for the first time that RhBG and RhCG transport not only  $\text{NH}_3$  but also  $\text{CO}_2$  (Figure 2, Figure 4). Bakouh et al performed one preliminary experiment on a  $\text{H}_2\text{O}$ -injected oocyte and one on a RhCG-expressing oocyte in which they monitored intracellular pH ( $\text{pH}_\text{i}$ ) while exposing the cells to a solution containing  $\text{CO}_2$  (Bakouh et al. 2006). Their data are consistent with the hypothesis that RhCG increase the rate of  $\text{CO}_2$ -induced fall in  $\text{pH}_\text{i}$ . We are aware of no reports concerning the  $\text{CO}_2$  permeability of RhBG. Han et al point out that RhBG and RhCG, although present in the bronchial epithelium of the lung, are absent from alveoli and thus are not in a position to contribute to  $\text{CO}_2$  transport (Han et al. 2009). However, they did not examine the  $\text{CO}_2$  permeabilities of the two Rh proteins.

Second, we find that the mutation of the conserved aspartate residues in RhBG (D178N) or RhCG (D177N) substantially reduces the abundance of the channel protein in the oocyte plasma membrane (Figure 3). Consistent with this interpretation, we find that the mutation of RhBG results in the near-total loss of the high-MW product that presumably represents mature, glycosylated RhBG. Others had proposed that these residues play a role in the deprotonation of  $\text{NH}_4^+$  (Javelle et al. 2004; Marini et al. 2006). Our data do not allow us to address the deprotonation hypothesis, inasmuch as the surface abundance of the mutant RhBG and RhCG is so low as to preclude the detection of channel-mediated transport. Our

data do support the proposal of Gruswitz et al. (2010) that the mutation of the residues would cause a structural disruption.

The RhBG cDNA used in the present study is the original human full-length clone (Lopez et al. 2005). Recently, Han et al. (2013) described a new variant of human RhBG, caused by a deletion of a single cytosine base, resulting in a frame shift in which residues 425–441 (17 aa) are replaced by new residues 425–459 (35 aa). Because the N terminus and the entire transmembrane spanning domains are unaffected, we think it is likely that the permeability properties of the original and new forms of RhBG are identical. The implications of the new variant for trafficking and regulation remain to be explored.

### Gas channels

The dogma had been that all gases freely diffuse through all membranes simply by dissolving into and diffusing through the lipid phase of the membrane. However, numerous publications have challenged this view. The first evidence challenging the diffusion of gases across membranes came from the observation that apical membranes of gastric-gland cells are impermeable to CO<sub>2</sub> and NH<sub>3</sub> (Waisbren et al. 1994), and apical membranes of colonic crypts are impermeable to NH<sub>3</sub> (Singh et al. 1995). The second piece of evidence challenging the dogma was the identification of the first family of gas channels, with the demonstration that AQP1, heterologously expressed in *Xenopus* oocytes, can conduct CO<sub>2</sub> (Nakhoul et al. 1998; Cooper and Boron 1998). In these experiments, the authors used as an index of CO<sub>2</sub> permeability the initial rate at which pH<sub>i</sub> declines (dpH<sub>i</sub>/dt). Because this dpH<sub>i</sub>/dt approach is somewhat insensitive, Nakhoul et al enhanced CO<sub>2</sub> influx by injecting CA II protein into the oocytes, whereas Cooper and Boron dissected away the vitelline membrane. Neither of these auxiliary maneuvers is necessary with the pH<sub>S</sub> approach used in the present study. Co-expression of CA II presumably would make the increase pH<sub>S</sub> to an extent in the present study, limited by the overall dynamic range of our system (solution changes, chamber, pH<sub>S</sub> electrode).

Later work showed that AQP1 also conducts NH<sub>3</sub> (Nakhoul et al. 2001) and nitric oxide (Herrera et al. 2006; Herrera and Garvin 2007). The rhesus proteins became the second known family of gas channels with the demonstration that they can conduct NH<sub>3</sub> (Ripoche et al. 2004). Work with red blood cells (RBCs) demonstrated that the Rh complex contributes CO<sub>2</sub> permeability (Endeward et al. 2008). We recently described a third family of gas channels, exemplified by the urea transporter UT-B, which conducts NH<sub>3</sub> (Geyer et al. 2013a). Moreover, work on AQPs and rhesus proteins expressed in *Xenopus* oocytes indicates that each channel has a characteristic selectivity for CO<sub>2</sub> vs. NH<sub>3</sub> (Musa-Aziz et al. 2009a; Geyer et al. 2013b).

The CO<sub>2</sub> permeability of plant aquaporins is important for providing CO<sub>2</sub> for photosynthesis (Uehlein et al. 2003; Kaldenhoff and Fischer 2006; Kaldenhoff 2012; Uehlein et al. 2012), and the CO<sub>2</sub> permeability of AQP1 (Endeward et al. 2006) is responsible for about half of the CO<sub>2</sub> permeability of RBCs.

Preliminary work shows that either the injection of CA II or the expression of CA IV increases both the maximal rate of pH<sub>i</sub> descent and pH<sub>S</sub> spike caused by CO<sub>2</sub> influx

(Musa-Aziz, Occhipinti & Boron, unpublished). The CA assays summarized in Figure 7a rule out the possibility that the enhanced  $\text{CO}_2$ -induced  $\text{pH}_\text{S}$  changes produced by RhAG, RhBG, and RhCG are due to the CA activity of the rhesus proteins per se, or of endogenous oocyte proteins. Previous work (Musa-Aziz et al. 2009a) led to a similar conclusion for AQP1. Thus, we can conclude that—like several AQPs—the three rhesus proteins examined in the present study act as channels for  $\text{CO}_2$  and  $\text{NH}_3$ .

### Possible physiological roles of RhBG and RhCG

The ability of RhBG and RhCG to conduct both  $\text{CO}_2$  and  $\text{NH}_3$  is reminiscent of the gas-transport properties of the related erythroid rhesus protein, RhAG (Musa-Aziz et al. 2009a). In RBCs, the  $\text{CO}_2$  permeability of RhAG, could enhance the uptake of  $\text{CO}_2$  in systemic tissues, for delivery to the lung. Similarly, the  $\text{NH}_3$  permeability of RhAG could promote the uptake the  $\text{NH}_3$  from systemic tissues, for delivery to the liver for detoxification.

What roles do RhBG and RhCG play in the CD in acid-base homeostasis? Others have proposed that the  $\text{NH}_3$  permeabilities of RhBG and RhCG are critical for  $\text{NH}_3/\text{NH}_4^+$  secretion during the defense against metabolic acidosis (Biver et al. 2008; Lee et al. 2009; Bishop et al. 2010; Gruswitz et al. 2010; Lee et al. 2010; Wagner et al. 2011; Weiner and Verlander 2011). Figure 8 summarizes the handling of  $\text{NH}_3/\text{NH}_4^+$  by the mTAL and CD. The mTAL reabsorbs  $\text{NH}_4^+$  via apical  $\text{Na/K/2Cl}$  cotransporters (with  $\text{NH}_4^+$  replacing  $\text{K}^+$ ), and  $\text{K}^+$  channels (Attmane-Elakeb et al. 2001). Inside the TAL cell,  $\text{NH}_4^+$  dissociates into  $\text{H}^+$  and  $\text{NH}_3$ . Via unknown mechanisms, the  $\text{NH}_3$  exits across the TAL basolateral membrane and enters the interstitial fluid of the renal medulla. A portion of this  $\text{NH}_3$  recycles back to the late PT and thin descending limb, some  $\text{NH}_3$  enters the blood stream for detoxification to urea in the liver, and the remaining  $\text{NH}_3$  passes through the basolateral and apical membranes of the collecting duct (CD) cell and enters the lumen, where it is trapped as  $\text{NH}_4^+$  and excreted in the urine. To the extent that  $\text{NH}_3/\text{NH}_4^+$  moves from the TAL lumen to the CD lumen, it bypasses the cortical segments of the distal nephron, where—due to the permeability of the cortical nephron segments to  $\text{NH}_3/\text{NH}_4^+$  and the greater blood flow of the cortex vs. the medulla—toxic quantities of  $\text{NH}_3/\text{NH}_4^+$  could otherwise escape into the blood. Moreover, any  $\text{NH}_4^+$  that escapes into the blood represents a net loss of urinary  $\text{NH}_3/\text{NH}_4^+$  that would compromise acid-base balance.

The sustained formation of  $\text{NH}_4^+$  in the CD lumen requires not only  $\text{NH}_3$  secretion across the apical membrane, but also  $\text{H}^+$  secretion to titrate the secreted  $\text{NH}_3$  to  $\text{NH}_4^+$ . This secreted  $\text{H}^+$  also titrates other luminal buffers, including some  $\text{HCO}_3^-$ . Regardless of what the secreted  $\text{H}^+$  titrates, an equivalent amount of  $\text{HCO}_3^-$  must exit the cell across the basolateral membrane of the CD cell via the renal form of AE1 (Romero 2005). The source of this cytosolic  $\text{HCO}_3^-$  is  $\text{CO}_2$ . The aforementioned models neither implicitly assume that  $\text{CO}_2$  can freely enter the collecting-duct cell across the basolateral membrane by an unspecified mechanism, or explicitly state that the  $\text{CO}_2$  enters by dissolving in the lipid phase of the plasma membrane. We propose that the bifunctional RhBG and RhCG channels in the CD are important not only for mediating  $\text{NH}_3$  uptake across the basolateral membrane but also for mediating  $\text{CO}_2$  uptake. Moreover, to the extent that the  $\text{H}^+$  secreted into the CD lumen titrates a small amount of luminal  $\text{HCO}_3^-$  to form  $\text{CO}_2$ , this  $\text{CO}_2$  could enter the aIC

via apical RhCG. Thus, the RhBG and RhCG would enhance CO<sub>2</sub> uptake into the αIC, thereby speeding luminal H<sup>+</sup> secretion.

## Conclusions

Our results confirm the observation that the human Rhesus family of transporters—namely RhAG, RhBG, and RhCG—exhibit significant permeability to NH<sub>3</sub> and show for the first time that RhBG and RhCG can conduct CO<sub>2</sub>. We could not assess the effect of specific Asp to Asn mutations (equivalent to D160 in AmtB) on the CO<sub>2</sub> and NH<sub>3</sub> permeability of RhBG and RhCG because these mutants have an extremely low abundance in the oocyte plasma membrane. Finally, we could not distinguish the CO<sub>2</sub>/NH<sub>3</sub> permeability ratios of RhAG, RhBG, and RhCG in this study.

## ACKNOWLEDGEMENTS

We thank Dale Huffman for computer support, Dr Alice Brown (University of Bristol) for plasmid cloning, and Dr. Nancy Amaral Rebouças (University of São Paulo) and Dr. Seong-Ki Lee for helpful discussions. RRG was supported by postdoctoral fellowship N00014-09-1-0246 from the Office of Naval Research. RMA was supported by Fundação de Amparo a Pesquisa do Estado de São Paulo (FAPESP # 08/128663). This work was supported by Office of Naval Research grant N00014-11-1-0889 and NIH grant DK81567 to WFB. AMT received funding from Kidney Research UK and NHS Blood and Transplant R&D.

## REFERENCES

- Attmane-Elakeb A, Amlal H, Bichara M (2001) Ammonium carriers in medullary thick ascending limb. *Am J Physiol Renal Physiol* 280:F1–9. [PubMed: 11133509]
- Bakouh N, Benjelloun F, Cherif-Zahar B, Planelles G (2006) The challenge of understanding ammonium homeostasis and the role of the Rh glycoproteins. *Transfus Clin Biol* 13:139–146. doi: 10.1016/j.traccli.2006.02.008 [PubMed: 16564724]
- Bishop JM, Verlander JW, Lee H-W, et al. (2010) Role of the Rhesus glycoprotein, Rh B glycoprotein, in renal ammonia excretion. *Am J Physiol Renal Physiol* 299:F1065–1077. doi: 10.1152/ajprenal.00277.2010 [PubMed: 20719974]
- Biver S, Belge H, Bourgeois S, et al. (2008) A role for Rhesus factor Rhcg in renal ammonium excretion and male fertility. *Nature* 456:339–343. doi: 10.1038/nature07518 [PubMed: 19020613]
- Boron WF, Boulpaep EL (1983) Intracellular pH regulation in the renal proximal tubule of the salamander. Basolateral HCO<sub>3</sub><sup>-</sup> transport. *J Gen Physiol* 81:53–94. [PubMed: 6833997]
- Brion LP, Schwartz JH, Zamilovitz BJ, Schwartz GJ (1988) Micro-method for the measurement of carbonic anhydrase activity in cellular homogenates. *Anal Biochem* 175:289–297. [PubMed: 3149875]
- Brown ACN, Hallouane D, Mawby WJ, et al. (2009) RhCG is the major putative ammonia transporter expressed in the human kidney, and RhBG is not expressed at detectable levels. *Am J Physiol Renal Physiol* 296:F1279–1290. doi: 10.1152/ajprenal.00013.2009 [PubMed: 19357182]
- Bruce LJ, Guizouarn H, Burton NM, et al. (2009) The monovalent cation leak in overhydrated stomatocytic red blood cells results from amino acid substitutions in the Rh-associated glycoprotein. *Blood* 113:1350–1357. doi: 10.1182/blood-2008-07-171140 [PubMed: 18931342]
- Cooper GJ, Boron WF (1998) Effect of pCMBS on CO<sub>2</sub> permeability of *Xenopus* oocytes expressing aquaporin 1 or its C189S mutant. *Am J Physiol* 275:C1481–1486. [PubMed: 9843709]
- Eldari D, Cheval L, Quentin F, et al. (2002) Expression of RhCG, a new putative NH<sub>3</sub>/NH<sub>4</sub><sup>+</sup> transporter, along the rat nephron. *J Am Soc Nephrol* 13:1999–2008. [PubMed: 12138130]
- Endeward V, Cartron J-P, Ripoché P, Gros G (2008) RhAG protein of the Rhesus complex is a CO<sub>2</sub> channel in the human red cell membrane. *FASEB J* 22:64–73. doi: 10.1096/fj.07-9097com [PubMed: 17712059]

- Endeward V, Musa-Aziz R, Cooper GJ, et al. (2006) Evidence that aquaporin 1 is a major pathway for CO<sub>2</sub> transport across the human erythrocyte membrane. *FASEB J* 20:1974–1981. doi: 10.1096/fj.04-3300com [PubMed: 17012249]
- Geyer RR, Musa-Aziz R, Enkavi G, et al. (2013a) Movement of NH<sub>3</sub> through the Human Urea Transporter B (UT-B): A New Gas Channel. *Am J Physiol Renal Physiol*. doi: 10.1152/ajprenal.00609.2012
- Geyer RR, Musa-Aziz R, Qin X, Boron WF (2013b) Relative CO<sub>2</sub>/NH<sub>3</sub> selectivities of mammalian Aquaporins 0–9. *Am J Physiol, Cell Physiol*. doi: 10.1152/ajpcell.00033.2013
- Giebisch G, Windhager EE (2009) Urine Concentration and Dilution In: Boron WF, Boulpaep EL (eds) *Medical Physiology. A Cellular and Molecular Approach*, 2nd ed. Elsevier Saunders, Philadelphia, PA, pp 835–850
- Gruswitz F, Chaudhary S, Ho JD, et al. (2010) Function of human Rh based on structure of RhCG at 2.1 Å. *Proc Natl Acad Sci USA* 107:9638–9643. doi: 10.1073/pnas.1003587107 [PubMed: 20457942]
- Han K-H, Croker BP, Clapp WL, et al. (2006) Expression of the ammonia transporter, Rh C glycoprotein, in normal and neoplastic human kidney. *J Am Soc Nephrol* 17:2670–2679. doi: 10.1681/ASN.2006020160 [PubMed: 16928804]
- Han K-H, Lee H-W, Handlogten ME, et al. (2013) Expression of the ammonia transporter family member, Rh B Glycoprotein, in the human kidney. *Am J Physiol Renal Physiol* 304:F972–981. doi: 10.1152/ajprenal.00550.2012 [PubMed: 23324176]
- Han K-H, Mekala K, Babida V, et al. (2009) Expression of the gas-transporting proteins, Rh B glycoprotein and Rh C glycoprotein, in the murine lung. *Am J Physiol Lung Cell Mol Physiol* 297:L153–163. doi: 10.1152/ajplung.90524.2008 [PubMed: 19429772]
- Herrera M, Garvin JL (2007) Novel role of AQP-1 in NO-dependent vasorelaxation. *Am J Physiol Renal Physiol* 292:F1443–1451. doi: 10.1152/ajprenal.00353.2006 [PubMed: 17229677]
- Herrera M, Hong NJ, Garvin JL (2006) Aquaporin-1 transports NO across cell membranes. *Hypertension* 48:157–164. doi: 10.1161/01.HYP.0000223652.29338.77 [PubMed: 16682607]
- Javelle A, Severi E, Thornton J, Merrick M (2004) Ammonium sensing in *Escherichia coli*. Role of the ammonium transporter AmtB and AmtB-GlnK complex formation. *J Biol Chem* 279:8530–8538. doi: 10.1074/jbc.M312399200 [PubMed: 14668330]
- Kaldenhoff R (2012) Mechanisms underlying CO<sub>2</sub> diffusion in leaves. *Curr Opin Plant Biol* 15:276–281. doi: 10.1016/j.pbi.2012.01.011 [PubMed: 22300606]
- Kaldenhoff R, Fischer M (2006) Aquaporins in plants. *Acta Physiol (Oxf)* 187:169–176. doi: 10.1111/j.1748-1716.2006.01563.x [PubMed: 16734753]
- Kim H-Y, Verlander JW, Bishop JM, et al. (2009) Basolateral expression of the ammonia transporter family member Rh C glycoprotein in the mouse kidney. *Am J Physiol Renal Physiol* 296:F543–555. doi: 10.1152/ajprenal.90637.2008 [PubMed: 19129254]
- Lee H-W, Verlander JW, Bishop JM, et al. (2010) Effect of intercalated cell-specific Rh C glycoprotein deletion on basal and metabolic acidosis-stimulated renal ammonia excretion. *Am J Physiol Renal Physiol* 299:F369–379. doi: 10.1152/ajprenal.00120.2010 [PubMed: 20462967]
- Lee H-W, Verlander JW, Bishop JM, et al. (2009) Collecting duct-specific Rh C glycoprotein deletion alters basal and acidosis-stimulated renal ammonia excretion. *Am J Physiol Renal Physiol* 296:F1364–1375. doi: 10.1152/ajprenal.90667.2008 [PubMed: 19321595]
- Lopez C, Métral S, Eladari D, et al. (2005) The ammonium transporter RhBG: requirement of a tyrosine-based signal and ankyrin-G for basolateral targeting and membrane anchorage in polarized kidney epithelial cells. *J Biol Chem* 280:8221–8228. doi: 10.1074/jbc.M413351200 [PubMed: 15611082]
- Ludewig U (2004) Electroneutral ammonium transport by basolateral rhesus B glycoprotein. *J Physiol (Lond)* 559:751–759. doi: 10.1113/jphysiol.2004.067728 [PubMed: 15284342]
- Mak D-OD, Dang B, Weiner ID, et al. (2006) Characterization of ammonia transport by the kidney Rh glycoproteins RhBG and RhCG. *Am J Physiol Renal Physiol* 290:F297–305. doi: 10.1152/ajprenal.00147.2005 [PubMed: 16131648]



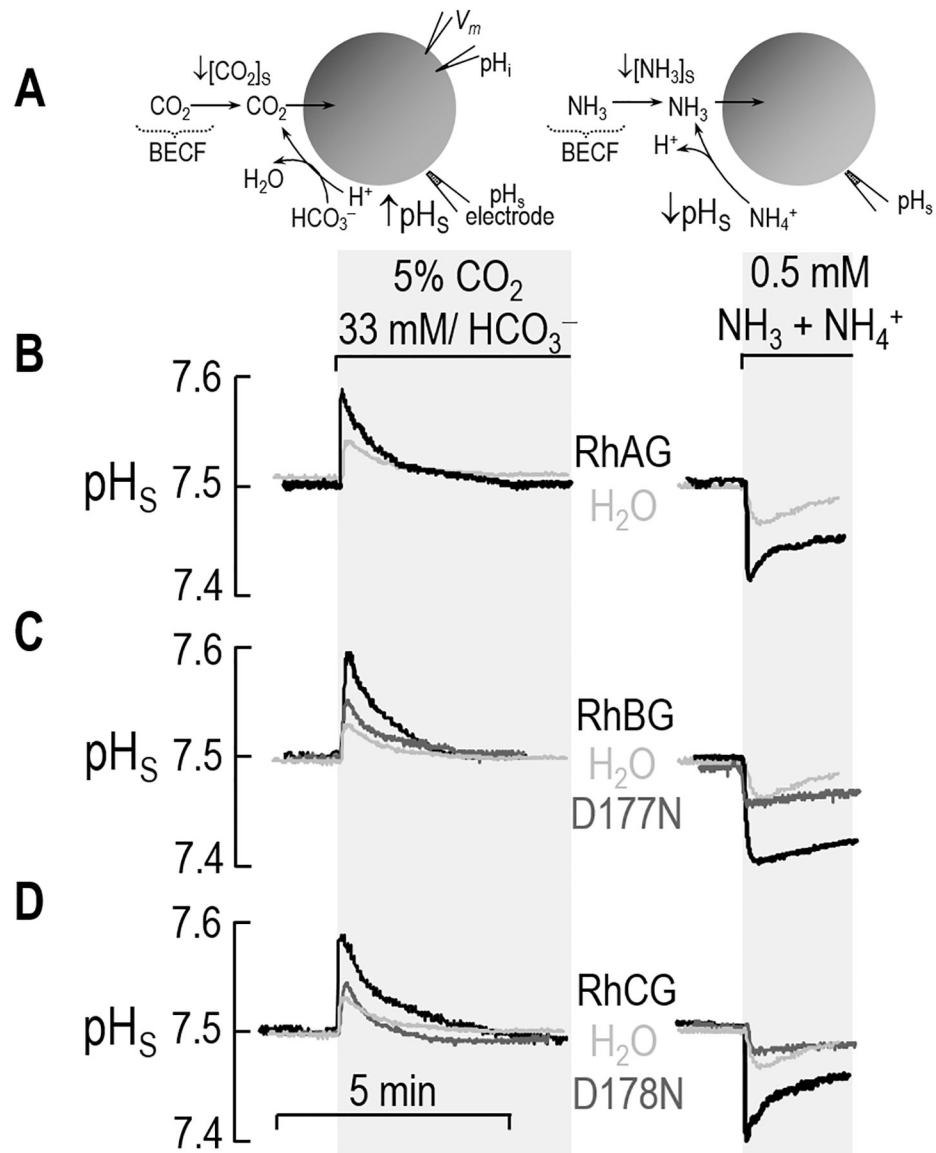
- Marini AM, Boeckstaens M, Benjelloun F, et al. (2006) Structural involvement in substrate recognition of an essential aspartate residue conserved in Mep/Amt and Rh-type ammonium transporters. *Curr Genet* 49:364–374. doi: 10.1007/s00294-006-0062-5 [PubMed: 16477434]
- Musa-Aziz R, Boron WF, Parker MD (2010) Using fluorometry and ion-sensitive microelectrodes to study the functional expression of heterologously-expressed ion channels and transporters in *Xenopus* oocytes. *Methods* 51:134–145. doi: 10.1016/j.ymeth.2009.12.012 [PubMed: 20051266]
- Musa-Aziz R, Chen L-M, Pelletier MF, Boron WF (2009a) Relative CO<sub>2</sub>/NH<sub>3</sub> selectivities of AQP1, AQP4, AQP5, AmtB, and RhAG. *Proc Natl Acad Sci USA* 106:5406–5411. doi: 10.1073/pnas.0813231106 [PubMed: 19273840]
- Musa-Aziz R, Grichtchenko II, Boron WF (2005) Evidence from surface-pH transients that CA IV & CA II enhances CO<sub>2</sub> influx into *Xenopus* oocytes. *J Am Soc Nephrol* 16:TH-PO016.
- Musa-Aziz R, Jiang L, Chen L-M, et al. (2009b) Concentration-dependent effects on intracellular and surface pH of exposing *Xenopus* oocytes to solutions containing NH<sub>3</sub>/NH<sub>4</sub><sup>+</sup>. *J Membr Biol* 228:15–31. doi: 10.1007/s00232-009-9155-7 [PubMed: 19242745]
- Nagami GT (1988) Luminal secretion of ammonia in the mouse proximal tubule perfused in vitro. *J Clin Invest* 81:159–164. doi: 10.1172/JCI113287 [PubMed: 3121674]
- Nakhoul NL, Davis BA, Romero MF, Boron WF (1998) Effect of expressing the water channel aquaporin-1 on the CO<sub>2</sub> permeability of *Xenopus* oocytes. *Am J Physiol* 274:C543–548. [PubMed: 9486145]
- Nakhoul NL, Hering-Smith KS, Abdunour-Nakhoul SM, Hamm LL (2001) Transport of NH<sub>3</sub>/NH<sub>4</sub><sup>+</sup> in oocytes expressing aquaporin-1. *Am J Physiol Renal Physiol* 281:F255–263. [PubMed: 11457716]
- Occhipinti R, Musa-Aziz R, Boron WF (2012) Mathematical modeling of the role of carbonic anhydrase II and IV on the influx of CO<sub>2</sub> in a *Xenopus* oocyte. *FASEB J* 26:882.9. [PubMed: 22075646]
- Quentin F, Eladari D, Cheval L, et al. (2003) RhBG and RhCG, the putative ammonia transporters, are expressed in the same cells in the distal nephron. *J Am Soc Nephrol* 14:545–554. [PubMed: 12595489]
- Ripoche P, Bertrand O, Gane P, et al. (2004) Human Rhesus-associated glycoprotein mediates facilitated transport of NH<sub>3</sub> into red blood cells. *Proc Natl Acad Sci USA* 101:17222–17227. doi: 10.1073/pnas.0403704101 [PubMed: 15572441]
- Ripoche P, Goossens D, Devuyt O, et al. (2006) Role of RhAG and AQP1 in NH<sub>3</sub> and CO<sub>2</sub> gas transport in red cell ghosts: a stopped-flow analysis. *Transfus Clin Biol* 13:117–122. doi: 10.1016/j.tracli.2006.03.004 [PubMed: 16574458]
- Romero MF (2005) Molecular pathophysiology of SLC4 bicarbonate transporters. *Curr Opin Nephrol Hypertens* 14:495–501. [PubMed: 16046910]
- Romero MF, Hediger MA, Boulpaep EL, Boron WF (1997) Expression cloning and characterization of a renal electrogenic Na<sup>+</sup>CO<sub>3</sub><sup>-</sup> cotransporter. *Nature* 387:409–413. doi: 10.1038/387409a0 [PubMed: 9163427]
- Seshadri RM, Klein JD, Kozlowski S, et al. (2006) Renal expression of the ammonia transporters, Rhbg and Rhcg, in response to chronic metabolic acidosis. *Am J Physiol Renal Physiol* 290:F397–408. doi: 10.1152/ajprenal.00162.2005 [PubMed: 16144966]
- Singh SK, Binder HJ, Geibel JP, Boron WF (1995) An apical permeability barrier to NH<sub>3</sub>/NH<sub>4</sub><sup>+</sup> in isolated, perfused colonic crypts. *Proc Natl Acad Sci USA* 92:11573–11577. [PubMed: 8524806]
- Somersalo E, Occhipinti R, Boron WF, Calvetti D (2012) A reaction-diffusion model of CO<sub>2</sub> influx into an oocyte. *J Theor Biol* 309:185–203. doi: 10.1016/j.jtbi.2012.06.016 [PubMed: 22728674]
- Toye AM, Williamson RC, Khanfar M, et al. (2008) Band 3 Courcouronnes (Ser667Phe): a trafficking mutant differentially rescued by wild-type band 3 and glycophorin A. *Blood* 111:5380–5389. doi: 10.1182/blood-2007-07-099473 [PubMed: 18174378]
- Uehlein N, Lovisolo C, Siefritz F, Kaldenhoff R (2003) The tobacco aquaporin NtAQP1 is a membrane CO<sub>2</sub> pore with physiological functions. *Nature* 425:734–737. doi: 10.1038/nature02027 [PubMed: 14520414]

- Uehlein N, Sperling H, Heckwolf M, Kaldenhoff R (2012) The Arabidopsis aquaporin PIP1;2 rules cellular CO<sub>2</sub> uptake. *Plant Cell Environ* 35:1077–1083. doi: 10.1111/j.1365-3040.2011.02473.x [PubMed: 22150826]
- Verlander JW, Miller RT, Frank AE, et al. (2003) Localization of the ammonium transporter proteins RhBG and RhCG in mouse kidney. *Am J Physiol Renal Physiol* 284:F323–337. doi: 10.1152/ajprenal.00050.2002 [PubMed: 12388412]
- Wagner CA, Devuyst O, Belge H, et al. (2011) The rhesus protein RhCG: a new perspective in ammonium transport and distal urinary acidification. *Kidney Int* 79:154–161. doi: 10.1038/ki.2010.386 [PubMed: 20927037]
- Wagner CA, Devuyst O, Bourgeois S, Mohebbi N (2009) Regulated acid-base transport in the collecting duct. *Pflügers Arch* 458:137–156. doi: 10.1007/s00424-009-0657-z [PubMed: 19277700]
- Waisbren SJ, Geibel JP, Modlin IM, Boron WF (1994) Unusual permeability properties of gastric gland cells. *Nature* 368:332–335. doi: 10.1038/368332a0 [PubMed: 8127367]
- Weiner ID, Verlander JW (2010) Molecular physiology of the Rh ammonia transport proteins. *Curr Opin Nephrol Hypertens* 19:471–477. doi: 10.1097/MNH.0b013e32833bfa4e [PubMed: 20539225]
- Weiner ID, Verlander JW (2011) Role of NH<sub>3</sub>/NH<sub>4</sub><sup>+</sup> transporters in renal acid-base transport. *Am J Physiol Renal Physiol* 300:F11–23. doi: 10.1152/ajprenal.00554.2010 [PubMed: 21048022]
- Zidi-Yahiaoui N, Mouro-Chanteloup I, D'Ambrosio A-M, et al. (2005) Human Rhesus B and Rhesus C glycoproteins: properties of facilitated ammonium transport in recombinant kidney cells. *Biochem J* 391:33–40. doi: 10.1042/BJ20050657 [PubMed: 15929723]

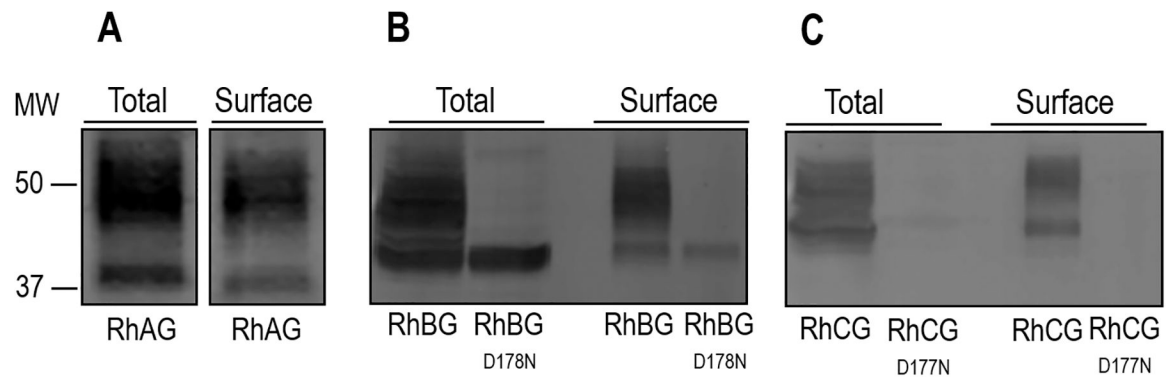
**AmtB**     $-G_{151}LLASHGALD_{160}FAGGTVVHI_{169}-$   
**RhAG**     $-I_{158}LLNLLKVKD_{167}AGGSMTIHT_{176}-$   
**RhBG**     $-V_{169}LLHLLGVVD_{178}AGGSMTIHT_{187}-$   
**RhCG**     $-L_{168}VSEIFKASD_{177}IGASMTIHA_{186}-$

**Figure 1.**

Multiple sequence alignment of RhAG, RhBG, and RhCG. Using CLUSTALW, a sequence alignment was generated to illustrate the conserved aspartate group in AmtB, RhAG, RhBG, and RhCG. The residue D160 in AmtB (Javelle et al. 2004) and the homologous D177 in RhCG (Marini et al. 2006) have been reported to be critical for NH<sub>3</sub> transport. This residue is also conserved in RhAG and RhBG. The WT sequence used for AmtB was Swissprot P69681. GenBank accession numbers for the other proteins were AF031548 (RhAG), AF193807 (RhBG), and AF193809 (RhCG).

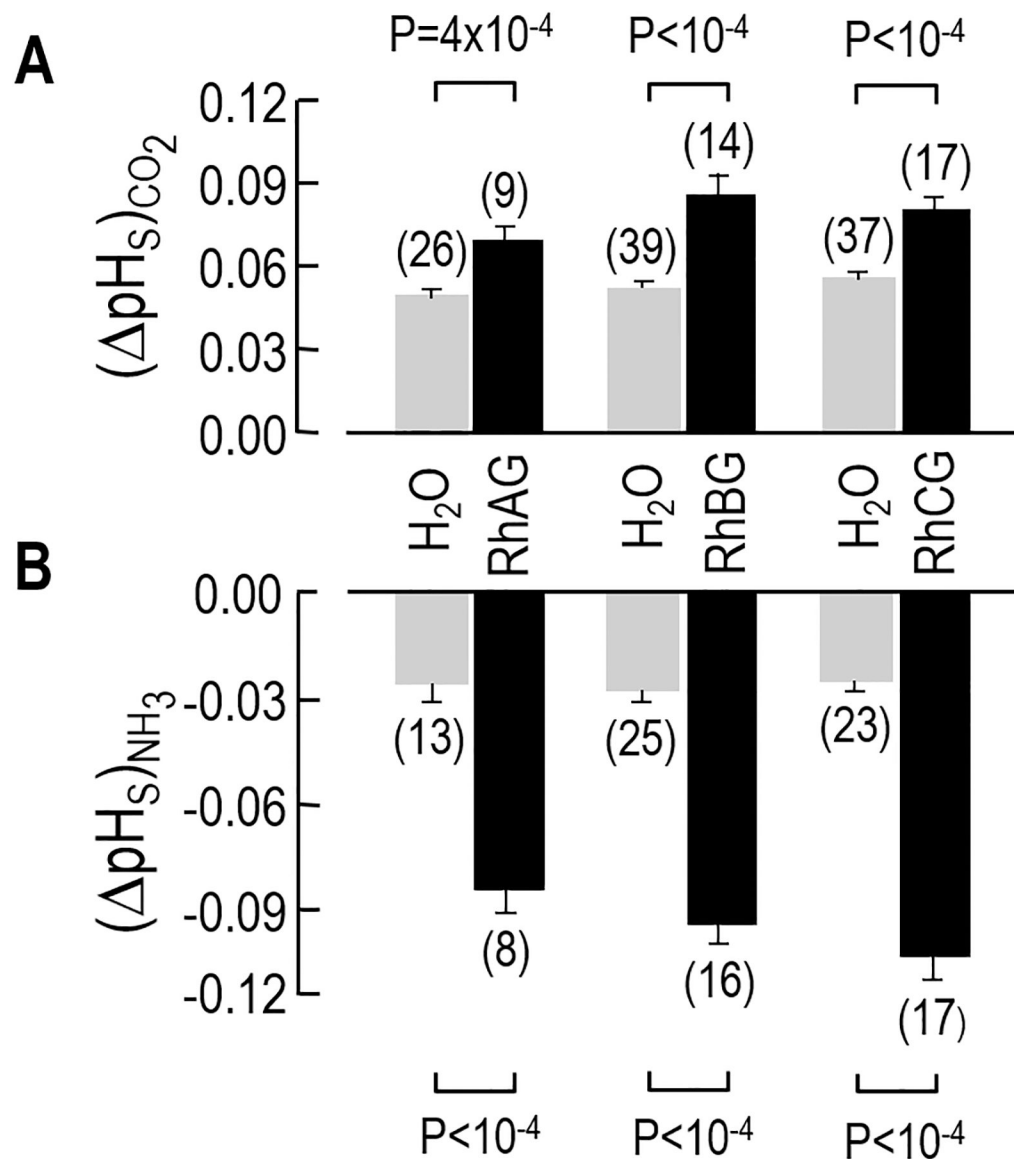
**Figure 2.**

Surface pH ( $\text{pH}_s$ ) measurements in oocytes exposed to  $\text{CO}_2/\text{HCO}_3^-$  or  $\text{NH}_3/\text{NH}_4^+$ . **a** Cell models. **b** RhAG and  $\text{H}_2\text{O}$ . **c** RhBG, RhBG<sub>D178N</sub>, and  $\text{H}_2\text{O}$ . **d** RhCG, RhCG<sub>D177N</sub>, and  $\text{H}_2\text{O}$ . In each experiment, the same oocyte is sequentially exposed to ND96, the 5%  $\text{CO}_2$ /33 mM  $\text{HCO}_3^-$  solution, ND96 again, and then finally the 0.5 mM  $\text{NH}_3/\text{NH}_4^+$  solution. During the exposure,  $\text{pH}_s$  measurements are recorded throughout the course of the experiment. We expose the oocyte to  $\text{CO}_2/\text{HCO}_3^-$  for a period of time long enough for the  $\text{pH}_s$  to rise and then decay to a stable value. Then following the washout of  $\text{CO}_2/\text{HCO}_3^-$  (~15 min, long enough for  $\text{pH}_i$  to stabilize), the same oocyte is then exposed to  $\text{NH}_3/\text{NH}_4^+$ . Routinely, we move the electrode away from the surface of the oocyte to calibrate it in the bath solution.



**Figure 3.**

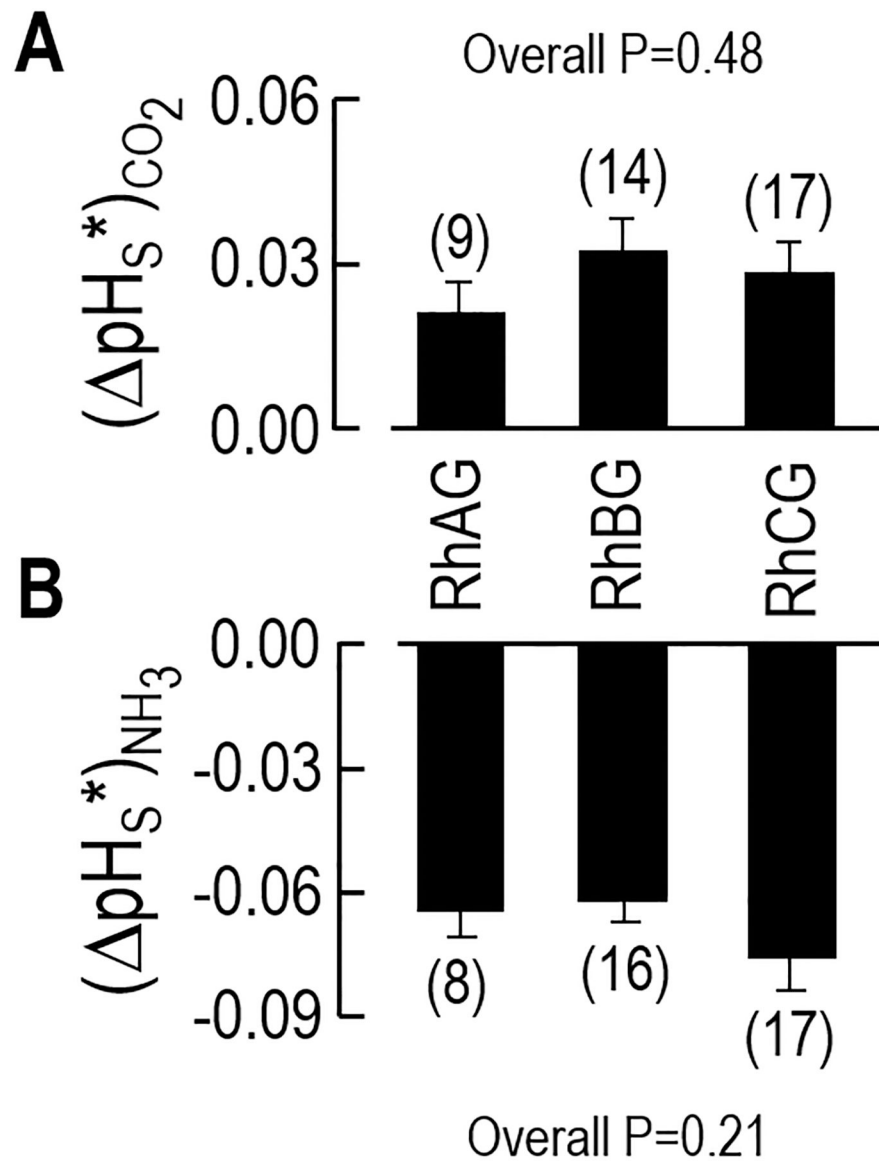
Surface expression of RhAG, RhBG, RhBG<sub>D178N</sub>, RhCG, and RhCG<sub>D177N</sub>. We assessed the total and surface expression of RhAG, RhBG, RhBG, RhBG<sub>D177N</sub>, RhCG, and RhCG<sub>D178N</sub> by biotinylating 30 intact oocytes injected with cRNA for each protein channel, and used anti-RhAG, anti-RhBG, or anti-RhCG to detect protein abundance. **a** RhAG. We detect the protein in both the total and surface fractions. There is also a characteristic high molecular weight pattern consistent with mature N-linked glycosylation in both samples. **b** RhBG. We also detect glycosylated WT RhBG in both total and surface fractions. However, the abundance of RhBG<sub>D178N</sub> in the total fraction is greatly reduced and lacks any detectable glycosylation. The abundance of the mutant protein is also greatly reduced at the cell surface. **c** RhCG. We detect WT protein in the total and surface fractions, but we are unable to detect appreciable amounts of RhCG<sub>D177N</sub> in either fraction. Molecular weight (MW) markers are displayed to the left.



**Figure 4.**

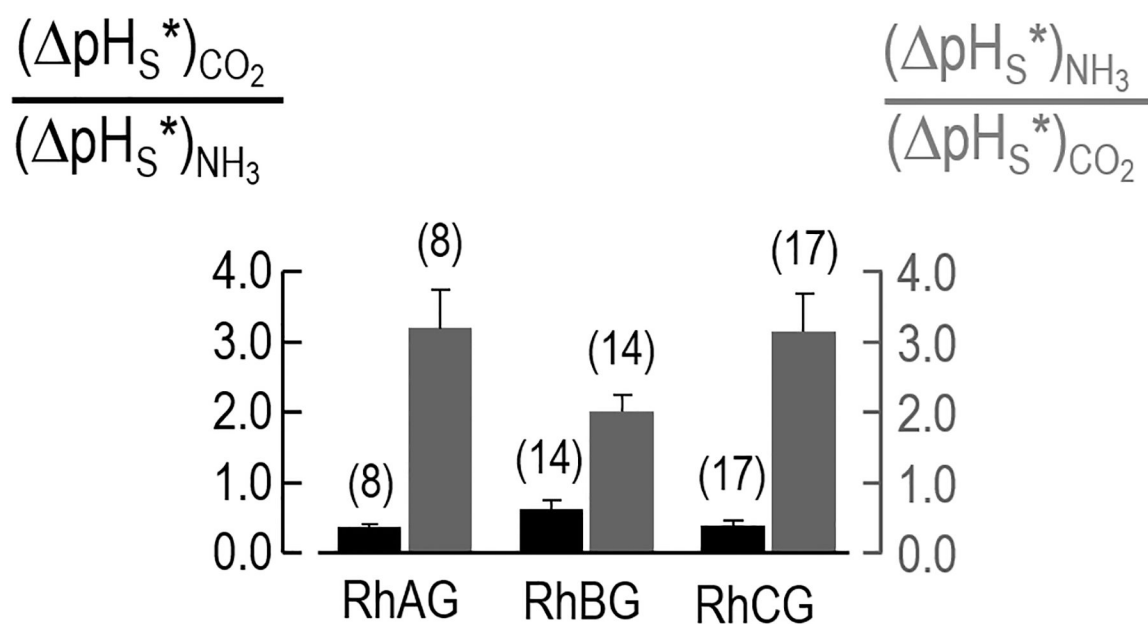
Data summary for the  $\text{pH}_S$  measurements. The bars summarize the results of a larger number of experiments, like those shown in Figure 2. **a** Maximum  $\text{pH}_S$  excursions evoked by  $\text{CO}_2$  exposure. Upon exposure to a flowing solution of 5%  $\text{CO}_2/33 \text{ mM HCO}_3^-$ ,  $\text{H}_2\text{O}$ -injected control oocytes become more alkaline. However, in the oocytes expressing RhAG, RhBG, or RhCG, the alkalization—as shown by a larger  $(\text{pH}_S)_{\text{CO}_2}$  value—is greater than that of  $\text{H}_2\text{O}$  injected oocytes. **b** Maximum  $\text{pH}_S$  excursions evoked by  $\text{NH}_3$  exposure. When the same oocyte is exposed to  $0.5 \text{ mM NH}_3/\text{NH}_4^+$ , the magnitude of the acidification  $(\text{pH}_S)_{\text{NH}_3}$  in the RhAG-, RhBG-, or RhCG-expressing oocytes is also greater than in  $\text{H}_2\text{O}$ -injected control oocytes. For RhBG<sub>D178N</sub> and the RhCG<sub>D177N</sub> the  $(\text{pH}_S)_{\text{CO}_2}$  and  $(\text{pH}_S)_{\text{NH}_3}$  values (not shown) are not statistically different from the  $\text{H}_2\text{O}$  injected controls. We performed Student's t-test (two tails) for statistical comparisons.





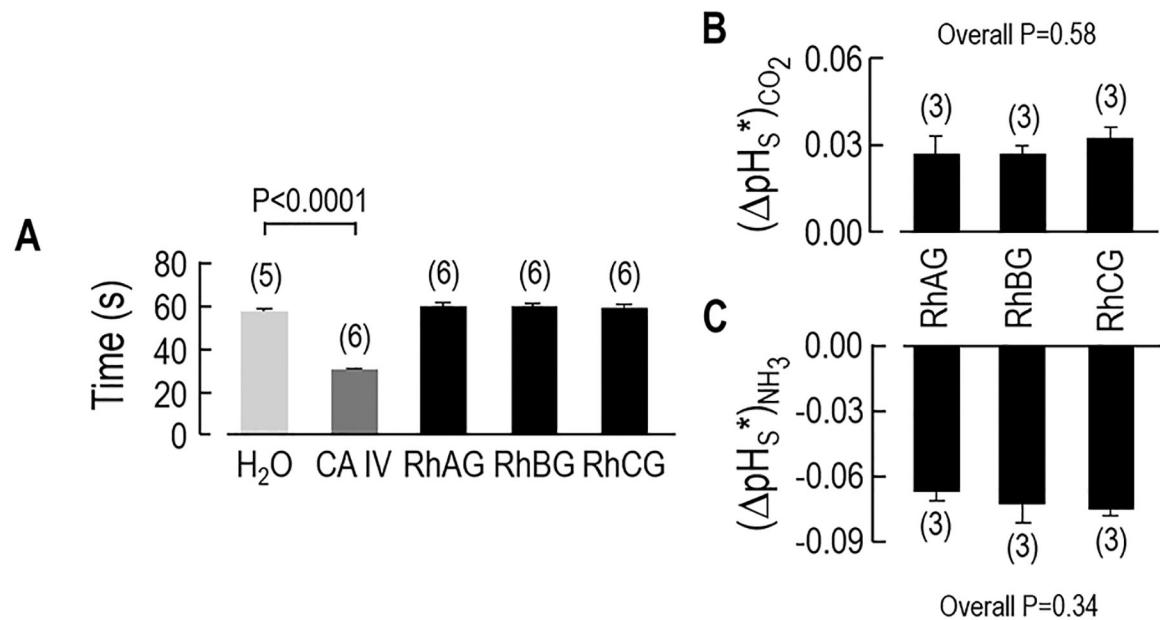
**Figure 5.**

Index of channel-dependent permeability to CO<sub>2</sub> or NH<sub>3</sub>. **a** Channel-dependent  $pH_S$  for CO<sub>2</sub>. **b** Channel-dependent  $pH_S$  for NH<sub>3</sub>. By subtracting the  $(pH_S)_{CO_2}$  or  $(pH_S)_{NH_3}$  for the H<sub>2</sub>O-injected control oocytes (see Figure 4) from the  $(pH_S)_{CO_2}$  or  $(pH_S)_{NH_3}$  of RhAG-, RhBG-, or RhCG-expressing oocytes (see Figure 4), we obtain  $(pH_S^*)_{CO_2}$ , a semiquantitative index of channel-dependent CO<sub>2</sub> permeability, or  $(-pH_S^*)_{NH_3}$ , a semiquantitative index of channel-dependent NH<sub>3</sub> permeability. In all cases, the  $pH_S$  values are significantly different from zero. However, the  $(pH_S^*)_{CO_2}$  values are similar for RhAG, RhBG, and RhCG; the same is true for the  $(-pH_S^*)_{NH_3}$  values. We did not compute these values for RhBG<sub>D178N</sub> and RhCG<sub>D177N</sub>, inasmuch as these proteins are not expressed at the oocyte membrane surface. We performed a 1-way ANOVA to assess statistical significance.



**Figure 6.**

Gas selectivity of RhAG, RhBG, and RhCG. Using the data underlying Figure 5, we calculated an index of relative CO<sub>2</sub>/NH<sub>3</sub> permeability ratio by dividing, oocyte by oocyte, (  $\Delta\text{pH}_S^*$ )<sub>CO<sub>2</sub></sub> by (  $\Delta\text{pH}_S^*$ )<sub>NH<sub>3</sub></sub> or (  $\Delta\text{pH}_S^*$ )<sub>NH<sub>3</sub></sub> by (  $\Delta\text{pH}_S^*$ )<sub>CO<sub>2</sub></sub>.

**Figure 7.**

Assessing the carbonic-anhydrase activity of oocytes expressing Rh proteins. **a** Colorimetric assays of carbonic-anhydrase activity of membrane preparations created from oocytes injected with H<sub>2</sub>O (negative control) or 12 ng/oocyte of cRNA encoding CA IV (positive control) or 25 ng/oocyte of cRNA encoding RhAG, RhBG, or RhCG. The value on the y axis indicates the time necessary for the color to change. We injected 100 oocytes of each type, made a membrane preparation of each group, and then repeated the colorimetric assay the indicated number of times. Other experiments (not shown) revealed that the time to the color change (~30 s) was the same after injecting either 25 ng cRNA/oocyte or 0.25 ng/oocyte. **b** Channel-dependent  $pH_s$  for CO<sub>2</sub> addition in 3 oocytes from the same batch of oocytes used in panel 'a'. **c** Channel-dependent  $pH_s$  for NH<sub>3</sub> addition for the same 3 oocytes as in panel 'b'. Values are means  $\pm$  SE, with nos. of oocytes in parentheses. For panel **a**, we performed Student's t-test (two tails) for statistical comparisons and for panel **b** and **c**, we performed one-way ANOVA, followed by Student-Newman-Keuls analyses.

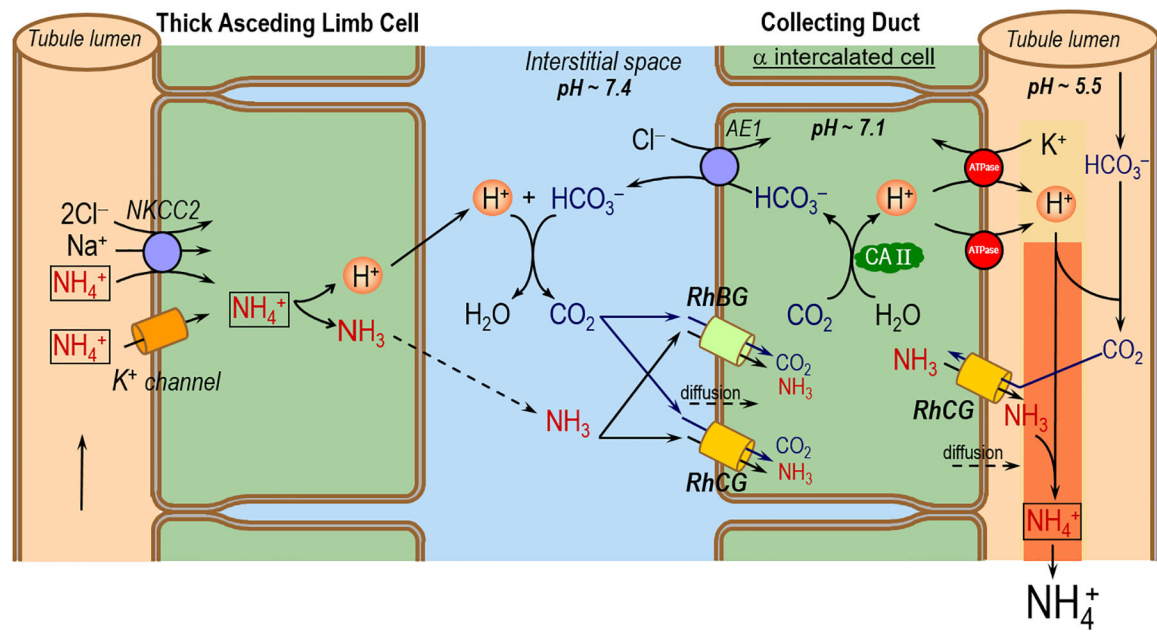


**Figure 8.**

Proposed novel model for CO<sub>2</sub> and NH<sub>3</sub> transport across the basolateral and apical membranes of αIC cell in the CD. NKCC2 (Na-K-2Cl cotransporter). AE1 (chloride bicarbonate exchanger). CA II (carbonic anhydrase II). This mechanism, particularly the aspects related to CO<sub>2</sub> movements, is an extension to the models proposed by others (Gruswitz et al. 2010). The dashed arrows represent the possible diffusion of CO<sub>2</sub> or NH<sub>3</sub> across plasma membranes.